ELSEVIER

Journal of Chromatography A, 950 (2002) 175–182

JOURNAL OF CHROMATOGRAPHY A

www.elsevier.com/locate/chroma

Hyperlayer separation in hollow fiber flow field-flow fractionation: effect of membrane materials on resolution and selectivity

Byung Ryul Min[a], Seok Jin Kim[a], Kyu-Hong Ahn[b], Myeong Hee Moon[c,*]

[a]*Department of Chemical Engineering, Yonsei University, Seoul 120-749, South Korea*

[b]*Future Technology Research Division, Korean Institute of Science and Technology, Seoul, South Korea*

[c]*Department of Chemistry, Pusan National University, Kuemjeong-Ku, Pusan 609-735, South Korea*

Received 6 September 2001; received in revised form 3 January 2002; accepted 3 January 2002

Abstract

Hollow fiber flow FFF (HF FlFFF) has recently shown its capability to separate and characterize the size of submicrometer particles and has demonstrated the potential to be developed into a disposable flow FFF channel. In this work, HF FlFFF was used for the hyperlayer separation of micron-sized particles and the separation capability was examined by using various hollow fiber membrane materials (Polysulfones, cPVC, and PAN). From the experiments, PAN (polyacrylonitriles) showed an outstanding performance in particle separation compared to the other membranes. By orienting the fiber module in an upright direction, the upstream flow migration reduced band broadening of eluted peaks. When the efficiency of the PAN hollow fiber system was tested by varying the ratio of outflow-rate to radial flow-rate, it was found that optimum separation in hyperlayer HF FlFFF can be obtained at the ratio of about 6–7. From the examination of retention at or around steric inversion diameter, it was observed that experiments showed a good agreement with predictions by semi-empirical calculation. In hyperlayer HF FlFFF the diameter based selectivity values were shown to be 1.2–1.7 depending on the type of membranes and the field strength (the radial flow-rate) conditions.

Keywords: Hyperlayer separation; Hollow fiber flow field-flow fractionation; Resolution; Selectivity; Field-flow fractionation

1. Introduction

Hollow fiber flow field-flow fractionation (HF FlFFF), one of the flow FFF subtechniques, has shown its capability to separate and characterize particles and macromolecules [1–7]. Unlike the rectangular channel used in most FFF techniques, HF FlFFF uses a cylindrical channel made with a hollow fiber membrane. Sample components in HF FlFFF are separated by the axial flow moving along the fiber axis with the aid of a force generated by the radial flow passing through the porous wall of the fiber membrane. Since there is no influx from a secondary flow, an external force observed in a conventional symmetrical flow FFF channel, the flow movement in hollow fiber flow FFF channel is similar to an asymmetrical flow FFF channel in which flow introduced to the hollow fiber is divided into two parts: part of the flow penetrates the fiber wall as radial flow and the rest exits along the fiber

*Corresponding author. Tel.: +82-51-510-2265; fax: 82-51-516-7641.

E-mail address: mhmoon@hyowon.pusan.ac.kr (M.H. Moon).

0021-9673/02/$ – see front matter
PII: S0021-9673(02)00029-8

as axial flow. Therefore, a sample component is driven toward the inner wall of a fiber by the force of radial flow.

Separation in a hollow fiber FlFFF requires the pre-establishment of an equilibrium state for sample materials prior to the separation process. Like an asymmetrical flow FFF system, sample relaxation in HF FlFFF is achieved by a focusing/relaxation method which forces sample components to form a narrow sample band at a position slightly apart from the fiber inlet by using the two convergent focusing flow streams originating at the fiber inlet and outlet [2,6]. During the focusing/relaxation process, the field force generated by radial flow drives the sample components toward the fiber wall and this force is counterbalanced by the diffusion of sample components against the wall. Thus, a sample component will be located at an equilibrium position depending upon its diffusive property, such as its hydrodynamic radius. Once sample relaxation is completely achieved, the backward flow from the fiber outlet is reversed toward the inlet for separation. In the case of proteins, macromolecules, and submicrometer sized particles, a sample component having a low MW or small diameter has a higher diffusion than a larger sample, as well as an equilibrium that is located further away from the fiber wall; thus it will be eluted first. Therefore, the order of separation is made with increasing MW or particle sizes. This is the typical mode of separation, referred to as normal mode [8,9]. However, supramicron particles have a negligible influence of diffusion in finding their equilibrium and they are transported closer to the wall. When this occurs, a large diameter particle will be protruded to a faster streamline of parabolic flow than that a small particle is located and it will be migrated down the channel earlier. Thus, the order of separation is reversed, referred to as the steric mode [8,10]. It has been found from FFF experiments that steric particles do not migrate at the surface of channel wall and they are migrated at an elevated position from the wall due to role of hydrodynamic lift forces [10]. Moreover, in flow FFF it has been shown that a large diameter particle is eluted at a position further away from the wall than a small particle and this results in the increase of the diameter based selectivity [11,12]. In the latter case, it is referred to as the hyperlayer mode in which the gap distance between particle and the channel wall is larger than the particle radius.

The first attempt to use a hollow fiber as an alternative to flow FFF channel was studied by Lee et al. in 1974 [1] and the feasibility studies were followed with few works by examining the effect of ionic strengths of carrier solution, the properties of fiber membrane, and the possibility of separating proteins and macromolecules [2–5]. Since a hollow fiber flow FFF module can be made inexpensively, it has a great potential to be developed into a disposable type of flow FFF channel. However, it has not been widely examined due to the lack of various membrane materials and a relatively poor resolution for separation. Recent works have shown that the separation resolution can be greatly improved to the level which is normally achieved by a conventional rectangular channel system with optimization works [6,7]. All of these studies were focused on the normal mode of separation. The possibility of separating large particles (>1 μm) has not been evaluated for HF FlFFF. In this work, a capability of hyperlayer separation in HF FlFFF is evaluated by testing three different fiber materials. Separation efficiency and diameter based selectivity in hyperlayer HF FlFFF were examined by varying the ratio of outflow-rate to radial flow-rate.

2. Theory

Particle retention in hollow fiber flow FFF follows the basic principle of field-flow fractionation as discussed earlier. However, as shown in a previous work, mathematical expression of retention ratio in a cylindrical flow FFF channel such as hollow fiber can be expressed differently as [3]:

$$R \cong 4\lambda_{\mathrm{HF}} \quad (\text{valid when } \lambda_{\mathrm{HF}} \ll 0.02 \text{ for normal mode of HF FlFFF}) \tag{1}$$

while retention ratio for a typical FFF system having rectangular cross section is represented as $R \cong 6\lambda$. The dimensionless parameter, λ_{HF}, for hollow fiber system is expressed similarly to the conventional flow FFF system as [3]:

$$\lambda_{\mathrm{HF}} = \frac{D}{Ur_{\mathrm{f}}} \tag{2}$$

where D is the diffusion coefficient of a sample component, U the radial flow velocity at fiber wall, and r_f the radius of fiber. Eqs. (1) and (2) fit well with particles eluting at normal mode of separation. For particles eluting at $\lambda_{HF} > 0.2$, a more precise expression of retention ratio [6] must be used to avoid a possible error in calculation. In experiments, retention time, t_r, can be predicted from the basic relationship, $R = t^0/t_r$, where t^0 is the void time expressed with the following equation as:

$$t^0 = \frac{V^0}{\dot{V}_{rad}} \ln \frac{\dot{V}_{in}}{\dot{V}_{out}} \quad (3)$$

in which V^0 is the geometrical fiber volume ($= \pi r_f^2 L$, L: length of fiber), $\dot{V}_{rad} (= 2\pi r_f LU)$, $\dot{V}_{in}$and $\dot{V}_{out}$ are the volumetric rate of radial flow, inlet flow, and outlet flow, respectively. In the case of a focusing/relaxation process made at a point L_0, $\dot{V}_{in}$ at the nominator of logarithm in Eq. (3) must be substituted with $\dot{V}_{in} - (L_0/L)\,\dot{V}_{rad}$. Therefore retention time in HF FlFFF is calculated by using Eqs. (1)–(3) as:

$$t_r = \frac{r_f^2}{8D} \ln \left(\frac{\dot{V}_{in} - (L_0/L)\,\dot{V}_{rad}}{\dot{V}_{out}} \right) \quad (4)$$

However, in hyperlayer mode of separation in HF FlFFF, the retention ratio can be expressed as [7]:

$$R = 4\gamma \frac{a}{r_f} \quad (5)$$

where a is the particle radius and γ is the correction factor, an experimental value related to particle diameter, field strength, and linear flow velocity [7,13]. Similarly to rectangular channel systems, retention of supramicrometer sized particles in HF FlFFF is governed by the hydrodynamic lift forces which play an important role in lifting particles away from the wall. Due to the complicated properties of lift force phenomena, particle retention can not be simply predicted from theory yet. Therefore, a calibration procedure is used to obtain a relationship between the retention time, t_r, and particle's diameter, d, and this can be expressed with the following equation:

$$\log t_r = \log t_{r1} - S \log d \quad (6)$$

where t_{r1} is the exptrapolated retention time of a unit diameter and S is the diameter based selectivity which is defined as:

$$S = \left| \frac{d \log t_r}{d \log d} \right| \quad (7)$$

From the linear relationship shown in Eq. (6), it is possible to calculate a particle's diameter or particle diameter distribution of polydisperse particulate sample materials in hyperlayer HF FlFFF. In addition, the experimental parameters obtained from calibration can be used to predict a steric inversion diameter, d_i semi-empirically as [7]:

$$d_i = \left(\frac{4kTt_{r1}}{3\pi\eta r_f U t^0 S} \right)^{\frac{1}{1+S}} \quad (8)$$

where k is Boltzman distribution constant, T is temperature, and η the carrier viscosity. Typical steric inversion is known to occur at 0.4–0.8 μm for flow FFF [14] and 0.7–1.0 μm for sedimentation FFF [9]. An experimental steric inversion in a typical FlFFF system is observed at or around 0.5 μm, which is smaller than the diameter (around 1.0 μm) for sedimentation FFF (SdFFF). The decrease in inversion diameters observed by flow FFF is in part originated by the difference in diameter based selectivity of each subtechnique ($S = 1.1$–1.5 for FlFFF and 0.7–0.8 for SdFFF) at steric/hyperlayer mode [11,15]. However, a large shift in inversion diameter is caused by the difference in the dependency of retention time on particle diameter between the two techniques in normal mode. Theoretically, retention time in flow FFF is linearly dependent on particle diameter, but in SdFFF it is proportional to the third power of diameter in the normal mode of separation. The difference in diameter dependency is reflected to the exponent value of Eq. (8) as $(1/1 + S)$ for flow FFF and $(1/3 + S)$ for SdFFF [16]. Therefore, the steric inversion diameter for flow FFF is expected to be smaller than that of SdFFF in general.

3. Experimental

Membrane materials used for hollow fiber flow FFF module in this work are polysulfone (PSf), chlorinated polyvinylchloride (cPVC), and polyacrylonitrile (PAN). The fiber radius and the MW cutoff

Table 1
Type of hollow fiber membranes used in this study

Type of material	Cutoff MW	Fiber radius (μm)	Manufacturer
Polysulfone (PSf)	30 000	410	SKU, Korea
	100 000	410	SKU, Korea
Chlorinated PVC (cPVC)	50 000	440	Sambo, Korea
Polyacrylonitrile (PAN)	50 000	415	Sambo, Korea

values are listed in Table 1. The hollow fiber flow FFF module is prepared in the same way as described in the previous reports [6,7]. The length of fiber, *L*, is 24.0 cm. The hollow fiber module is oriented vertically so that particle migration is made in an upstream direction. The carrier liquid used for HF FlFFF is deionized water (>18 MΩ) containing 0.1% FL-70, a mixture of nonionic and anionic surfactant, from Fisher Scientific (Fair Lawn, NJ, USA) with 0.02% sodium azide as a bacteriocide. The carrier solution was delivered to the hollow fiber module using a model 930 HPLC pump from Younglin Instrument (Seoul, Korea). Sample materials used were polystyrene latex spheres having nominal diameters of 9.775, 6.992, 4.991, 4.000, 3.044, 2.013, 1.034, 0.806, 0.596, 0.426, 0.304, 0.204, 0.135, and 0.096 μm from Duke Scientific (Palo Alto, CA, USA). The density of PS latex standards is 1.05 g/cm^3. The first seven sizes referred to 10, 7, 5, 4, 3, 2, and 1 μm hereafter. Eluted particles were monitored at 254 nm by a model 720 UV detector from Younglin. Sample injection was made with a model 7125 loop injector from Rheodyne (Cotati, CA, USA) and was done with a reduced flow-rate of 0.5 ml/min through the fiber inlet. Once injected particles were expected to reach at or close to the point which is 10% of fiber length, the focusing/relaxation process was begun by delivering carrier solution through both the inlet and outlet of the fiber. The ratio of flow-rate from both inlet and outlet used for focusing/relaxation was adjusted as 1:9 so that sample components were focused at 0.1 l. The flow conversion was made by using both four- and three-way switching valves as illustrated in Fig. 1. After relaxation was completely achieved, the flow from the fiber outlet was reverted to fiber inlet and the separation was begun. The control of flow-rate was made with the model SS-SS2-VH metering valve from Nupro (Willoughby, OH, USA).

4. Results and discussion

Separation of supramicrometer sized particles by HF FlFFF was evaluated with three different hollow fiber membranes and the fractograms are shown in Figs. 2 and 3. Fig. 2 shows the separation of six different polystyrene latex beads obtained with (a) cPVC, (b) PSf-30 (cut-off MW: 30 K), and (c) PSf-100. All runs were made at a fixed run condition, $\dot{V}_{out}/\dot{V}_{rad} = 3.40/0.61$ in ml/min. For the hollow fibers used in Fig. 2, separation fractograms appear to be broad but they show a high speed separation typically observed in steric or hyperlayer

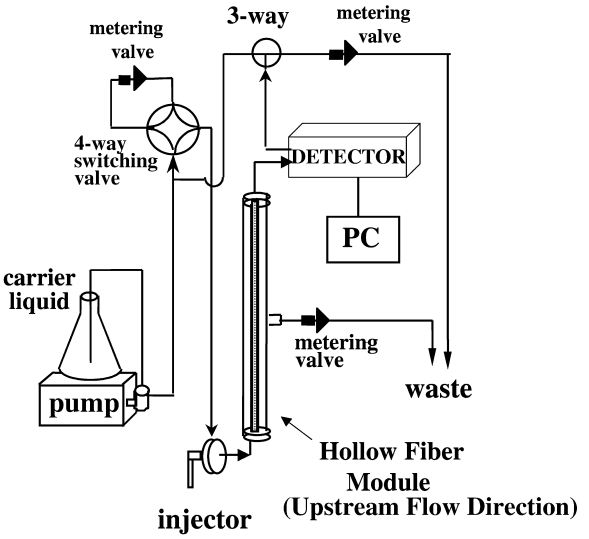

Fig. 1. System configuration of hollow fiber flow field-flow fractionation (HF FlFFF).

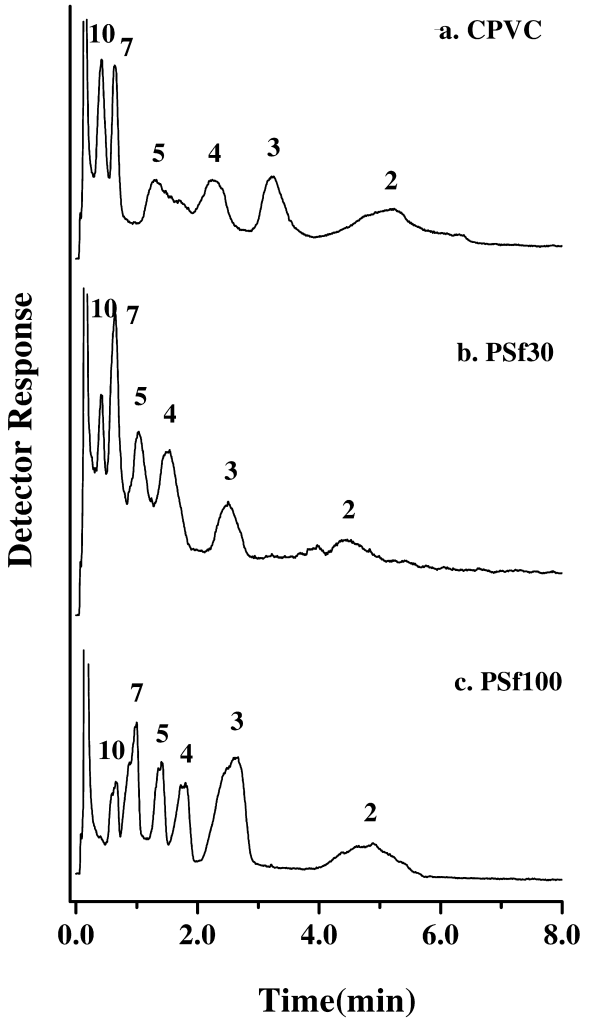

Fig. 2. Hyperlayer separation of six different polystyrene standards obtained with (a) cPVC, (b) PSf30, (c) PSf100 hollow fiber membranes by HF FlFFF. Experimental condition is fixed at $\dot{V}_{out}/\dot{V}_{rad}=3.40/0.61$ in ml/min.

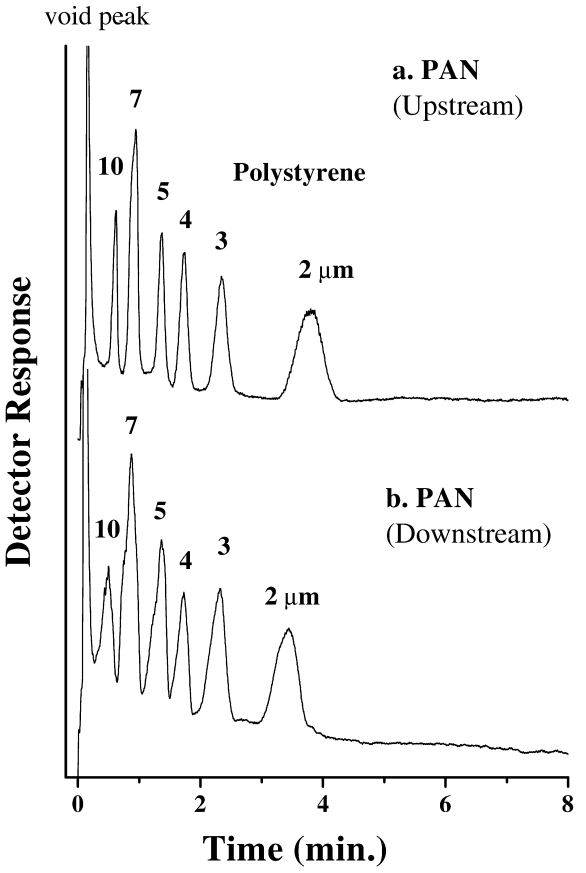

Fig. 3. Comparison of separation obtained by PAN hollow fiber membrane at two different flow orientations: (a) upstream and (b) downstream flow directions. Run condition is the same as used in Fig. 2.

operation of FFF techniques. However, the resolution shown in Fig. 2 is not as good as it was observed in conventional flow FFF system [12]. When a hollow fiber module made with PAN was used, the resolution was greatly improved by showing a baseline separation of all components in Fig. 3a. The separation fractogram in Fig. 3a demonstrates a great capability of HF FlFFF as an alternative separation technique for supramicron particles. The time period given for focusing/relaxation is 2.3 min. When the focusing period was increased to 8 min for test, there was no serious deterioration in the resolution observed. The fractograms in Figs. 2 and 3a were obtained with upstream configuration as shown in Fig. 1 so that particles migrated along the fiber to the opposite direction of the gravity field. When the fiber module was positioned in an opposite direction so that migrating flow moved downward, eluted peaks appeared to be slightly broad as shown in the fractogram of Fig. 3b. This may have arisen from an additional band broadening induced by gravity which can considerably affect the migrating band. In the case of diameter based selectivity, there was only a slight variation between the two conditions: $S=1.17$

(correlation coefficient is 0.999) for the upstream orientation and 1.22 (cc = 0.993) for the downstream orientation. Repeated runs of each calibration yield about less than 1% of a relative error in slope. From this observation, later works are carried out with the upstream flow orientation. From the experimental retention times of PS in Fig. 3a, γ (shown in Eq. (5)) values for each particle are calculated to be about 9–11 for PS 2–10 μm particles. Calculation of the gap distance between particle and the channel wall also shows that particles migrate at a distance much larger than the particle radius from the channel wall. This supports that retention mode observed in the current hollow fiber flow FFF is hyperlayer.

By using PAN as a source of hollow fiber module, diameter based selectivity was further examined at different flow-rate conditions. Fig. 4 shows a set of calibration curves, a plot of $\log t_r$ versus $\log d$, obtained (a) by varying outflow-rate under a fixed ratio of $\dot{V}_{out}/\dot{V}_{rad} = 8.0$ and (b) by varying the ratio under a fixed rate of outflow, $\dot{V}_{out} = 4.24$ ml/min. Calibration plots show a good linear relationship between logarithm of retention time and logarithm of diameter down to 2.0 μm polystyrene particles. The selectivity values calculated for each run condition are listed in Table 2 and they appear to vary from 1.14 to 1.35. When outflow-rate increases under the same ratio of $\dot{V}_{out}/\dot{V}_{rad}$ in Fig. 4a, selectivity gradually increases. However, selectivity increases when the ratio, $\dot{V}_{out}/\dot{V}_{rad}$, decreases under the same outflow-rate shown in Fig. 4b. Both experiments show that the hyperlayer effect on particle elution becomes larger when linear flow velocity increases; either by increasing outflow velocity or by increasing radial flow-rate. The variation in selectivity values was further studied with four different hollow fiber modules by varying radial flow-rate at a fixed outflow-rate of 3.44 ml/min. The calculated S values are listed in Table 3. While PAN shows the best separation resolution among the four membrane modules, as shown in Figs. 2 and 3, selectivity values for PAN fiber are relatively smaller than those (1.47–1.69) of PSf30, PSf100, and cPVC fibers.

Separation efficiency of a PAN hollow fiber module is examined with the measurement of plate height data by varying the ratio, $\dot{V}_{out}/\dot{V}_{rad}$, using PS 3 μm in Fig. 5. A minimum plate height is observed experimentally when the flow-rate ratio, $\dot{V}_{out}/\dot{V}_{rad}$, decreases to nearby 7.0 at outflow-rate conditions marked within the Fig. 5. The calculated number of experimental plates becomes about 720 at an out-

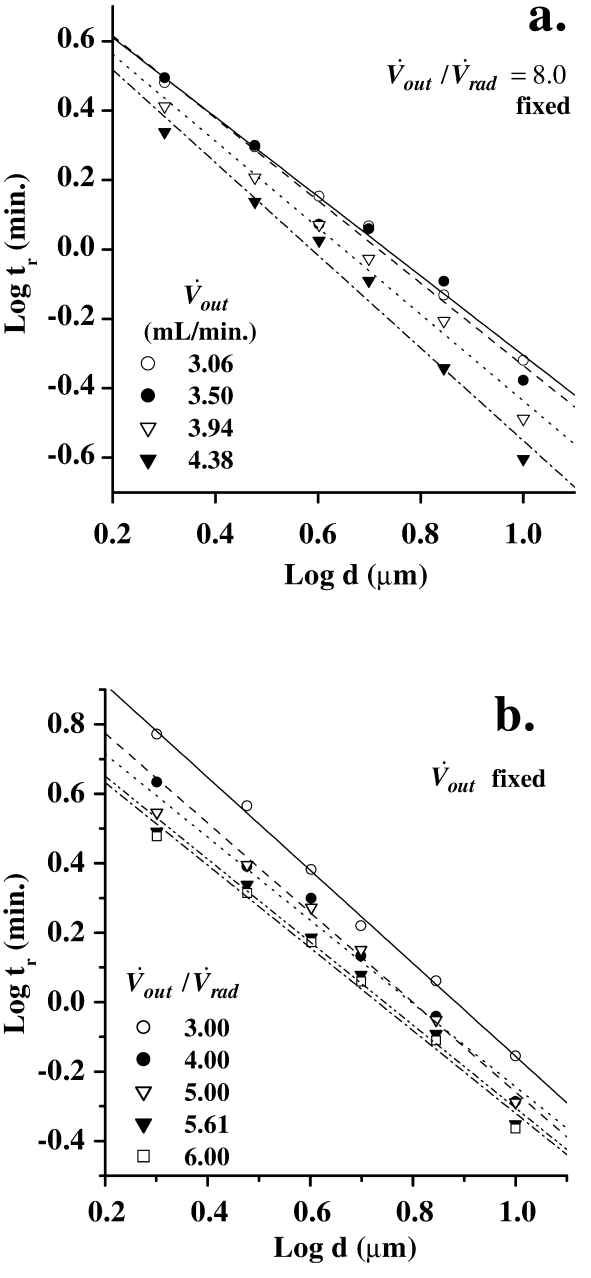

Fig. 4. A set of calibration plots showing a linear relationship obtained at (a) a fixed ratio of $\dot{V}_{out}/\dot{V}_{rad} = 8.0$ by varying outflow-rates (marked inside) and (b) a fixed outflow-rate ($\dot{V}_{out} = 4.24$ ml/min.) by varying the ratio, $\dot{V}_{out}/\dot{V}_{rad}$.

Table 2
Experimental run conditions and calibration parameters corresponding to the plots of Fig. 4 (all data were obtained with a PAN hollow fiber module)

$\dot{V}_{out}$ (ml/min)	$\dot{V}_{out}/\dot{V}_{rad}$	S	t_{r1} (min)	Correlation coefficient
3.06	8.0	1.14	6.91	0.999
3.50	8.0	1.19	7.13	0.988
3.94	8.0	1.21	6.20	0.997
4.38	8.0	1.34	6.09	0.991
4.24	3.0	1.35	15.40	0.999
4.24	4.0	1.29	10.84	0.997
4.24	5.0	1.20	9.02	0.992
4.24	5.6	1.20	7.76	0.994
4.24	6.0	1.19	7.43	0.994

flow-rate of 3.5 ml/min. When the ratio, $\dot{V}_{out}/\dot{V}_{rad}$, further decreases, experimental plate heights appear to increase again.

Steric inversion phenomenon in hollow fiber flow FFF was investigated with a series of PS standards having different diameters (0.050–10 μm). The measurement of elution times was made at two different run conditions: $\dot{V}_{out}/\dot{V}_{rad}=3.40/0.61$ and 1.42/0.15 in ml/min. Fig. 6 shows the plots of logarithm of retention time vs. logarithm of diameter obtained for 15 different PS standards. The two straight lines shown at the left side of Fig. 6 represent the theoretical retention times at normal mode calculated at each experimental condition using Eq. (4). The other two straight lines located at the right side of the figure are the steric calibration plots based on particles 2–10 μm. It is likely that a steric effect influences the elution of submicron particles since the retention times from the left side of Fig. 6 appear to be shorter than the calculated values (straight line) except few standards. Experimental data points start deviating further from the theory for the case of 0.204 μm (the fourth data point from the left). This is due to the increase of hydrodynamic lift forces as particle size becomes larger. A steric transition is observed around 0.3 and 0.4 μm for the two run conditions. Particles at or around the steric inversion regime appear to follow the center curve which is calculated by a combined retention equation of both normal and steric modes using calibration parameters. The inversion diameters calculated by using Eq. (8) are 0.26 and 0.38 μm for run conditions, $\dot{V}_{out}/\dot{V}_{rad}=3.40/0.61$ and 1.42/0.15 in ml/min, respectively. The experimental parameters used for the calculation are $S=1.46$ (cc = 0.998) and $t_{r1}=10.88$ min for $\dot{V}_{out}/\dot{V}_{rad}=3.40/0.61$, and $S=1.19$ (cc = 0.997) and $t_{r1}=13.66$ min for the latter run condition. It is noted that experimental observations agree well with the expectation that inversion diameter decreases with the decrease of t_{r1}

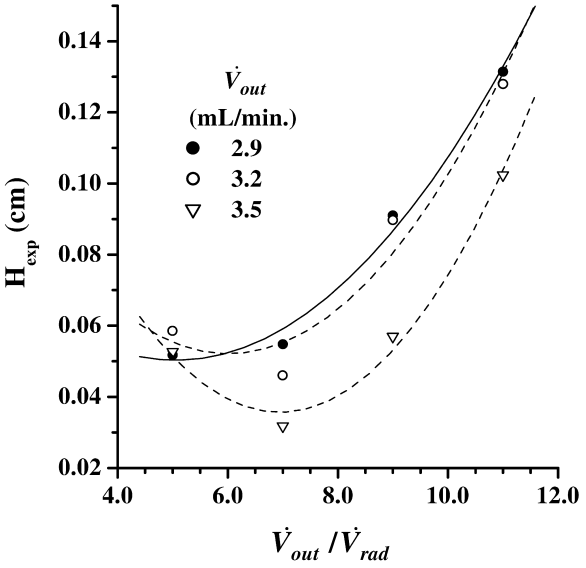

Fig. 5. Experimental plate heights obtained by varying $\dot{V}_{out}/\dot{V}_{rad}$ at three different outflow-rate conditions.

Table 3
List of selectivity values, S, depending on the type of hollow fiber membranes (outflow-rate is fixed at 3.44 ml/min)

Radial flow rate (ml/min)	PSf30		PSf100		cPVC		PAN	
	S	cc	S	cc	S	cc	S	cc
0.56	1.51	0.992	1.50	0.979	1.49	0.993	1.25	0.976
0.66	1.55	0.992	1.52	0.978	1.50	0.994	1.29	0.976
0.76	1.65	0.992	1.50	0.991	1.48	0.995	1.30	0.983
0.86	1.69	0.990	1.51	0.996	1.50	0.995	1.26	0.993

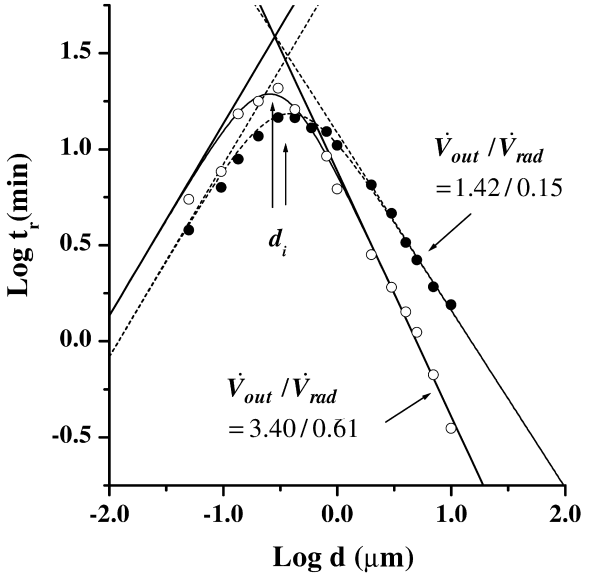

Fig. 6. Plots of $\log t_r$ *vs.* $\log d$ for polystyrene standards of 15 different sizes obtained at two different run conditions that are marked inside the figure. The steric inversion is clearly observed for each run condition.

and with the increase of radial flow velocity and selectivity.

In this study, HF FlFFF system has shown its potential to successfully separate supramicron particles. Examinations of the separation resolution and the diameter based selectivity of hyperlayer separation demonstrated that the performance of PAN hollow fiber is comparable to that of a conventional rectangular channel. It also shows that steric inversion diameter can be shifted to a smaller diameter by adjusting $\dot{V}_{out}/\dot{V}_{rad}$. However, the current works show a limitation in separating particles larger than 10 μm. A further study is needed to expand the dynamic span of size ranges by using a fiber of thicker radius or optimizations in flow-rates.

Acknowledgements

This work was partly supported by Green Korea21 from KIST.

References

[1] H.-L. Lee, J.F.G. Reis, J. Dohner, E.N. Lightfoot, AIChE J. 20 (1974) 776.
[2] J.A. Jönsson, A. Carlshaf, Anal. Chem. 61 (1989) 11.
[3] J.A. Jönsson, A. Carlshaf, J. Microcol. Sep. 3 (1991) 411.
[4] A. Carlshaf, J.A. Jönsson, Sep. Sci. Technol. 28 (1993) 1031.
[5] J.E.G.J. Wijnhoven, J.-P. Koorn, H. Pope, W.Th. Kok, J. Chromatogr. A 732 (1996) 307.
[6] W.J. Lee, B.-R. Min, M.H. Moon, Anal.Chem. 71 (1999) 3446.
[7] M.H. Moon, K.H. Lee, B.R. Min, J. Microcol. Sep. 11 (1999) 676.
[8] J.C. Giddings, Science 260 (1993) 1456.
[9] M. Schimpf, K.D. Caldwell, J.C. Giddings (Eds.), Field-Flow Fractionation Handbook, Wiley-Interscience, New York, 2000.
[10] K.D. Caldwell, T.T. Nguyen, M.N. Myers, J.C. Giddings, Sep. Sci. Technol. 14 (1979) 335.
[11] S.K. Ratanathanawongs, J.C. Giddings, Chromatographia 38 (1994) 545.
[12] M.H. Moon, K.-M. Kim, Y. Byun, D. Pyo, J. Liq. Chromatogr. Relat. Technol. 22 (1999) 2729.
[13] S. Lee, J.C. Giddings, Anal. Chem. 60 (1988) 2328.
[14] K.D. Jensen, S.K.R. Williams, J.C. Giddings, J. Chromatogr. A 746 (1996) 137.
[15] J.C. Giddings, M.H. Moon, P.S. Williams, M.N. Myers, Anal. Chem. 63 (1991) 1366.
[16] M.H. Moon, J.C. Giddings, Anal. Chem. 64 (1992) 3029.